



COMPARATIVE BLADES NUMBER HORIZONTAL AXIS WIND TURBINES IN PROFILE NACA 0012 USING CFD SIMULATION

DEWI PUSPITA SARI^{1,3*}, DJOKO SETYANTO¹, REXON H. SIMANJUNTAK¹, AHMAD ALFARIZI BARZAH², WADIRIN³, EDI SETIYO³, RUDI HERMAWAN³

¹Professional Engineer Certification, School of Bioscience, Technology, and Innovation, Atma Jaya Catholic University of Indonesia

²Department of Mechanical Engineering, Faculty of Engineering, Universitas Sriwijaya, South Sumatra, Indonesia

³Study Program of Mechanical Engineering Education, Faculty of Teacher Training and Education, Universitas Sriwijaya, South Sumatra, Indonesia

*Corresponding author: dewipuspita@fkip.unsri.ac.id

(Received: 11 February 2025; Accepted: 1 May 2025; Published on-line: 13 May 2025)

ABSTRACT: This study explores the effect of blade count on the performance of low-scale horizontal axis wind turbines (HAWT) with NACA 0012 profiles using Computational Fluid Dynamics (CFD) methods. The results show that the turbine with three blades achieves the highest efficiency, with a power coefficient (C_p) of 0.54 at a Tip-Speed Ratio (TSR) of 7, while the four-blade turbine reaches a C_p of 0.48 at a TSR of 6. The mechanical power produced by the three-blade turbine is 1,040.81 W, 28% higher than that of the four-blade turbine (927.28 W). The progressive distribution of the pitch angle in the three-blade turbine minimizes the risk of stall and flow separation. These findings suggest that fewer blades can reduce flow interference and vortex-induced losses, making it an efficient solution for the wind energy potential in Indonesia. Future research should explore geometric and material variations for further optimization.

KEY WORDS: HAWT; NACA 0012; blade number; CFD; tip-speed ratio.

1. INTRODUCTION (HEADING 1)

Electrical energy plays a crucial role in human activities, with per capita consumption in Indonesia increasing to 1,173 kWh in 2022 (up 4% from the previous year) [1]. However, electricity generation in Indonesia still relies on coal (67.21% in 2022) and faces distribution challenges in the archipelago [2].

On the other hand, wind energy offers significant potential with an average speed of 3-10 m/s and a power potential of around 978 MW [3], primarily through low-scale horizontal axis wind turbines (HAWT) (10-100 kW).

Wind turbine efficiency is influenced by blade design, airfoil selection, number of blades, and material [4], [5] The NACA 0012 airfoil is the leading choice due to its high efficiency and stability characteristics, which have been tested through Computational Fluid Dynamics (CFD) simulations [6]. Although the maximum efficiency of wind turbines is limited by Betz's law (59.3%) [7], optimization of parameters such as Tip-Speed Ratio (TSR), rotor speed, number of blades, and distribution of twist angles can approach optimal performance [8].

Previous studies have shown that the number of blades affects torque and aerodynamic efficiency. CFD simulation is key in analyzing fluid-structure interactions, especially for low scales with variable wind speeds [9][10]. In addition, balancing the load distribution through precise blade design can reduce drag and increase output power [11].

This study aims to study the effect of the number of HAWT blades with a low-scale NACA 0012 profile using the CFD method. The study's results are expected to be a reference for designing community-scale wind turbines that are adaptive to Indonesian wind conditions while supporting the diversification of renewable energy.

2. METHOD

This study uses analytical methods to design the blade geometry and computational methods based on Computational Fluid Dynamics (CFD) simulation with QBlade and ANSYS software.

2.1. Analytical Method

The analytical method aims to determine the turbine blade design parameters through the following aerodynamic equations. The theoretical wind power (P_o) available from the airflow is calculated by:

$$P_o = \frac{1}{2} \rho A v^3 \quad (W) \quad (1)$$

where ρ = air density (kg/m^3), A = rotor swept area (m^2), and v = wind speed (m/s).

The shaft angular speed (ω) is optimized based on Tip-Speed Ratio (λ):

$$\lambda = \frac{v_w}{v} = \frac{R \cdot \omega}{v} \text{ and } \omega = \lambda \cdot \frac{v_{wind}}{R} \quad (rad/s) \quad (2 - 3)$$

The local radius (r) distribution along the blade is determined by:

$$\lambda = r = r_{Hub} + \left[\left(\frac{R - r_{Hub}}{n} \right) \times elemen \right] \quad (4)$$

Local TSR (λ_r):

$$\lambda_r = \frac{r}{R} \times \lambda \quad (5)$$

The optimum λ value is seven based on the literature study [12]. The optimum chord length (C_{opt}) based on Betz momentum theory and relative velocity distribution:

$$C_{opt} = \frac{2\pi r}{z} \frac{8}{9C_L} \frac{v}{\lambda_r v_r} \quad (m) \quad (6)$$

The distribution of twist angle (θ) and pitch (β) is calculated from the geometric relationship of the velocity triangle (Figure 1):

$$\theta = \tan^{-1} \left(\frac{1}{\lambda_r} \right) \text{ and } \beta = \theta - \alpha \quad (7 - 8)$$

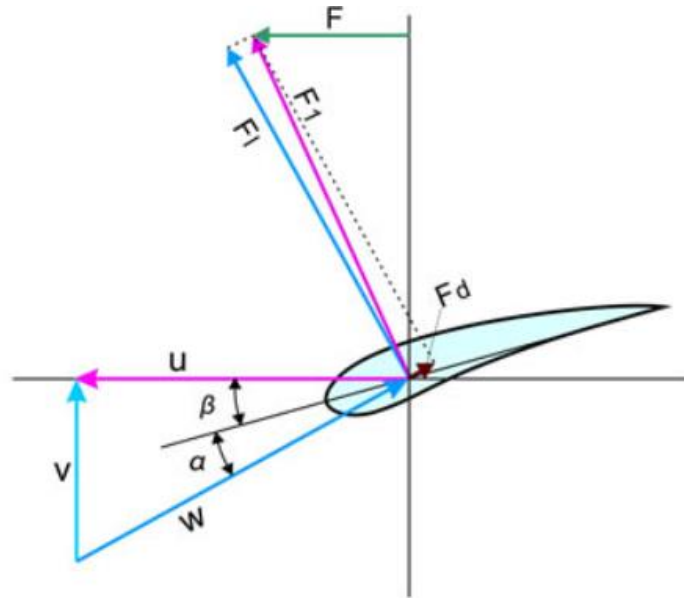


Fig. 1. Airfoil velocity triangle.

2.2. Computational Method

Simulation is carried out in two stages: Airfoil analysis with Qblade to determine the optimum lift (C_L) and drag (C_D) coefficients of the NACA 0012 profile at varying angles of attack (α). The CFD Simulation with ANSYS includes 3D Modeling for the turbine blades designed in SOLIDWORKS based on analytical parameters and exported to Parasolid format. Fluid Domain Creation: The rotational region is modeled as a cylinder with a radius of $5 \times$ the blade radius. The inlet and outlet planes are spaced $3.5 \times$ and $5.5 \times$ the blade radius, respectively, to minimize turbulence effects [13] (Figure 2).

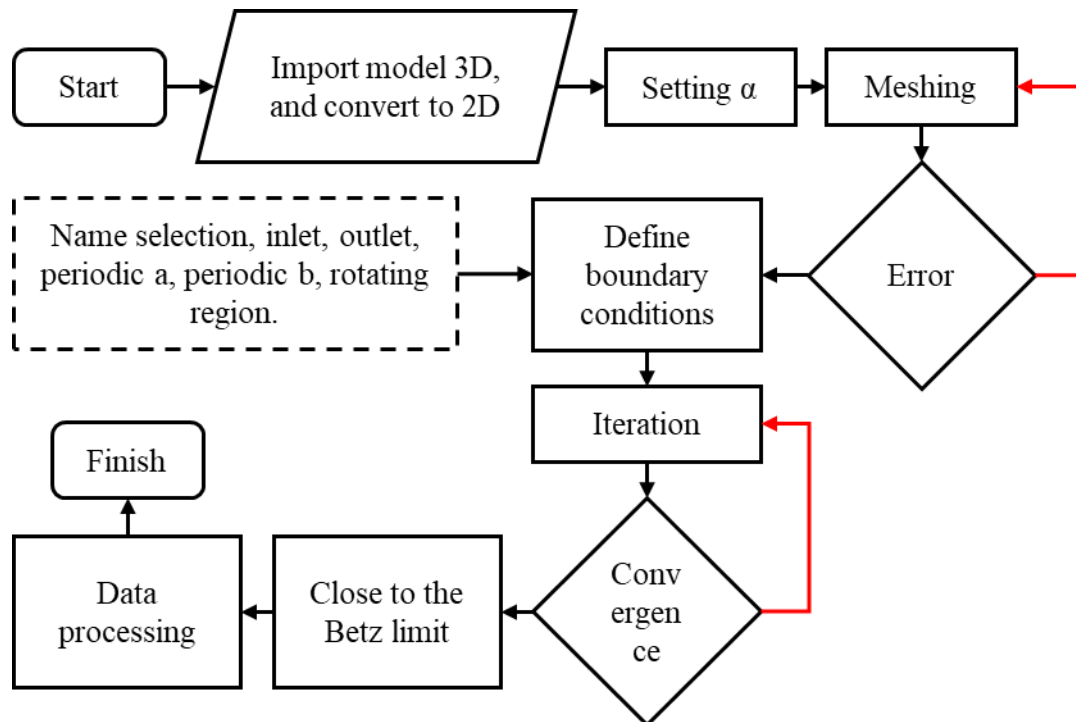


Fig. 2. Simulation flowchart.

Wind speed (v) and rotational velocity (ω) are set according to the simulation scenario for boundary condition setting. Turbulence is modeled with $k-\omega$ SST for near-wall flow accuracy [14]. Post-Processing: Torque and pressure distributions are analyzed to calculate the power coefficient (C_p).

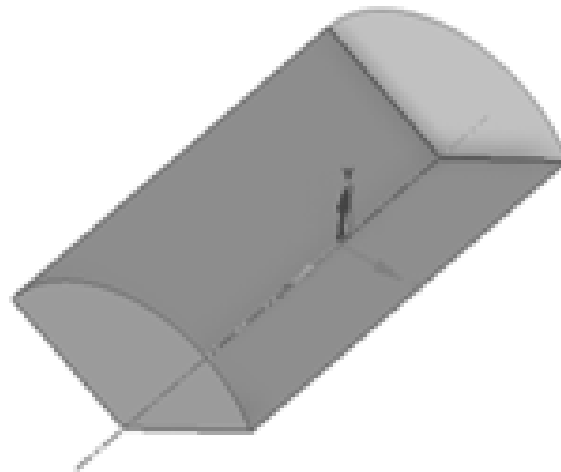


Fig. 3. Geometry of the wind tunnel boundary.

3. RESULTS AND DISCUSSION

This research analyzes the influence of the number of blades (3 and 4) on the performance of a low-scale NACA 0012 profile horizontal axis wind turbine (HAWT) through CFD simulations. Analytical and computational results are presented as follows:

3.1. Analytical Results

Geometry Distribution of Blades

Based on the Betz momentum equation and design parameters ($TSR = 7$ for 3 blades; $TSR = 6$ for 4 blades), the optimum chord lengths at each local radius are obtained (Table 1-2). The chord value decreases as the radius increases, with a similar pattern for both blade configurations.

Table 1: Optimum chord length of a 3-blade turbine

r_{local} (m)	Z	C_l	v_r (m/s)	C_{opt} (m)
0.150	3	0.868	14.5	0.2112
0.235			19.25	0.1591
0.320			24.53	0.1248
0.405			30.06	0.1019
0.490			35.72	0.0857
0.575			41.47	0.0738
0.660			47.26	0.0648
0.745			53.10	0.0577
0.830			58.95	0.0519
0.915			64.82	0.0472
1			70.71	0.0433



Table 2: Optimum chord length of 4-blade turbine

r_{local} (m)	Z	C_l	v_r (m/s)	C_{opt} (m)
0.150	4	0.868	13.45	0.2655
0.235			17.28	0.2067
0.320			21.64	0.1650
0.405			26.27	0.1359
0.490			31.05	0.1150
0.575			35.92	0.0994
0.660			40.84	0.0875
0.745			45.80	0.0780
0.830			50.79	0.0703
0.915			55.80	0.0640
1			60.82	0.0587

Torsion Angle Distribution

The torsion angle (θ) and pitch (β) are calculated based on the local TSR and the optimum angle of attack ($\alpha=7.5^\circ$). The 3-blade turbine has a flatter angle distribution than the 4-blade turbine (Table 3-4), reducing the stall risk at the hub radius.

Table 3: Torsion angle of 3-blade turbine

TSR_{local}	α ($^\circ$)	θ ($^\circ$)	β ($^\circ$)
1.05	7.5	43.60	36.10
1.645		31.30	23.80
2.24		24.06	16.56
2.835		19.43	11.93
3.43		16.25	8.75
4.025		13.95	6.45
4.62		12.21	4.71
5.215		10.85	3.35
5.81		9.77	2.27
6.405		8.87	1.37
7		8.13	0.63

Table 4: Torsion angle of 4-blade turbine

TSR_{local}	α ($^\circ$)	θ ($^\circ$)	β ($^\circ$)
0.9	7.5	48.01	40.51
1.41		35.35	27.85
1.92		27.51	20.01
2.43		22.37	14.87
2.94		18.79	11.29
3.45		16.16	8.66
3.96		14.17	6.67
4.47		12.61	5.11
4.98		11.35	3.85
5.49		10.32	2.82
6		9.46	1.96



3.2. Simulation Results

3.3.1. Turbine Performance Based on TSR

The simulation results show that the 3-blade turbine achieves a maximum power coefficient (C_p) of 0.54 at Tip-Speed Ratio (TSR) 7, while the 4-blade turbine achieves a C_p of 0.48 at TSR 6 (Table 5-6, Figure 4). The highest mechanical power is generated by the 3-blade configuration of 1,040.81 W at TSR 7, outperforming the 4-blade (927.28 W) by a difference of 28%. The decrease in efficiency at $TSR > 7$ is caused by an increase in drag due to airflow separation on the blade surface, which is reinforced by the visualization of denser vortices in the 4-blade turbine (Figure 8-9) [13]; this proves that the number of blades affects the aerodynamic load distribution, flow stability, and energy conversion efficiency.

Table 5: Performance of 3-blade turbine at TSR variation

λ	ω (rad/s)	τ (Nm)	P_o (W)	P_m (W)	C_p
3	30	0.58	1924	121.87	0.06
4	40	1.06		223.03	0.11
5	50	1.40		294.24	0.15
6	60	2.22		467.43	0.24
7	70	4.95		1040.81	0.54
9	90	3.52		740.35	0.38
11	110	1.60		336.86	0.17

Table 6: Performance of 4-blade turbine at TSR variation

λ	ω (rad/s)	τ (Nm)	P_o (W)	P_m (W)	C_p
3	30	0.42	1924	101.92	0.05
4	40	2.38		572.25	0.29
5	50	2.96		710.71	0.36
6	60	3.86		927.28	0.48
7	70	3.16		759.12	0.39
9	90	2.46		591.83	0.30
11	110	1.19		286.48	0.14

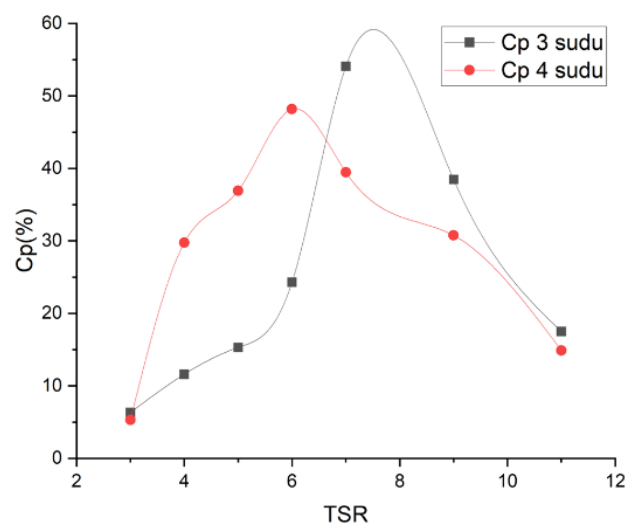


Fig. 4. TSR vs C_p .

3.3.2. Effect of Angle of Attack (α)

NACA 0012 shows optimum performance at $\alpha=7.5^\circ$ with the highest C_p (0.54 for 3 blades; 0.482 for 4 blades). Increasing $\alpha>7.5^\circ$ causes a decrease in C_L/C_D and stall (Table 7-8, Figure 5).

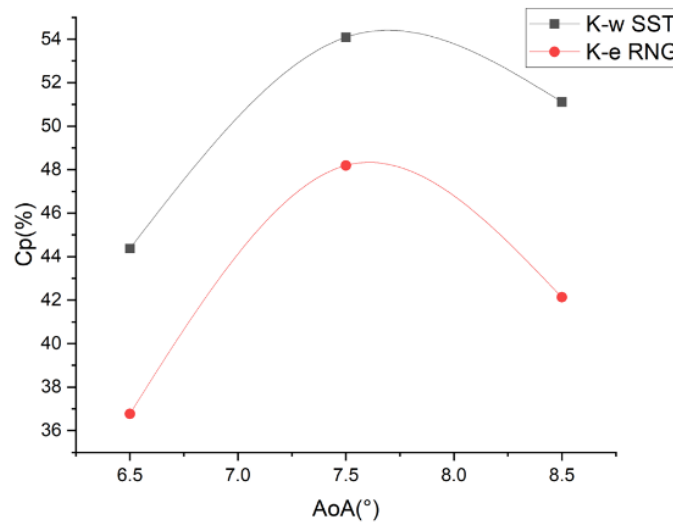


Fig. 5. α vs C_p .

Table 7: Simulation results for a 3-blade turbine at α variation

α ($^\circ$)	τ (Nm)	P_m (W)	C_p
6.5	4.0657	853.797	0.4437
7.5	4.95628	1040.819	0.5409
8.5	4.6832	983.472	0.5111

Table 8: Simulation results for a 4-blade turbine at α variation

α ($^\circ$)	τ (Nm)	P_m (W)	C_p
6.5	2.9483	707.592	0.368
7.5	3.8637	927.288	0.482
8.5	3.378	810.72	0.421

3.3. Visual CFD Analysis

3.3.1. Pressure and Velocity Distribution

CFD simulation results show the highest pressure distribution centered on the leading edge (Figure 6) at position $R/r=1$ m, with a stable pressure gradient along the 3-blade turbine blade.

This indicates that the optimal twist angle design can maintain laminar flow and reduce the risk of flow separation. Meanwhile, the velocity contour in Figure 7 shows a uniform airflow distribution on the blade surface, with minimization of separation bubbles—a phenomenon that generally reduces efficiency due to local turbulence.

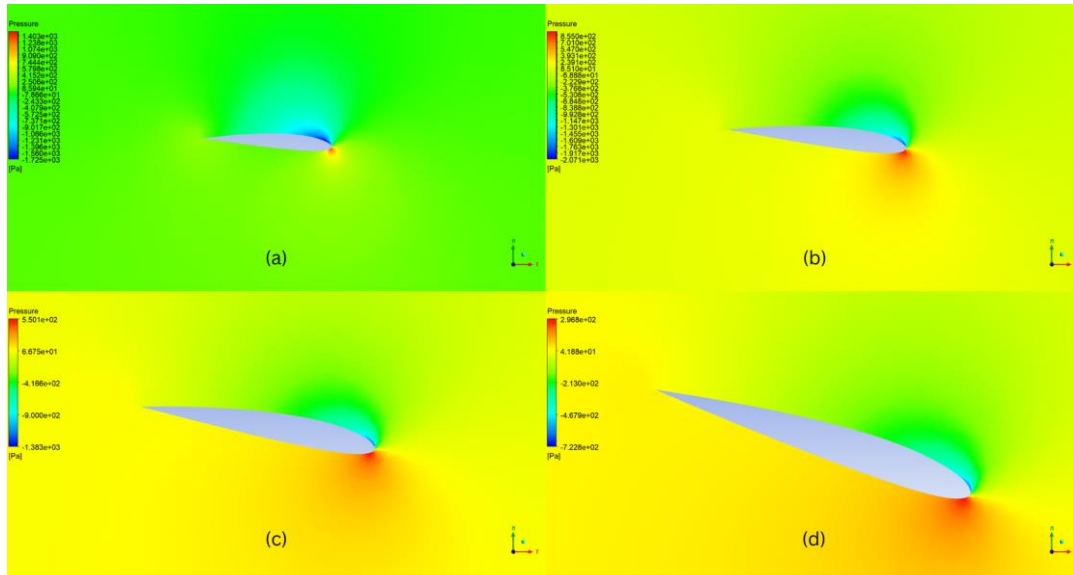


Fig. 6. Pressure contours on 3 blades a. R/r 1m b. R/r 0.75 m c. R/r 0.5 m d. R/r 0.25 m

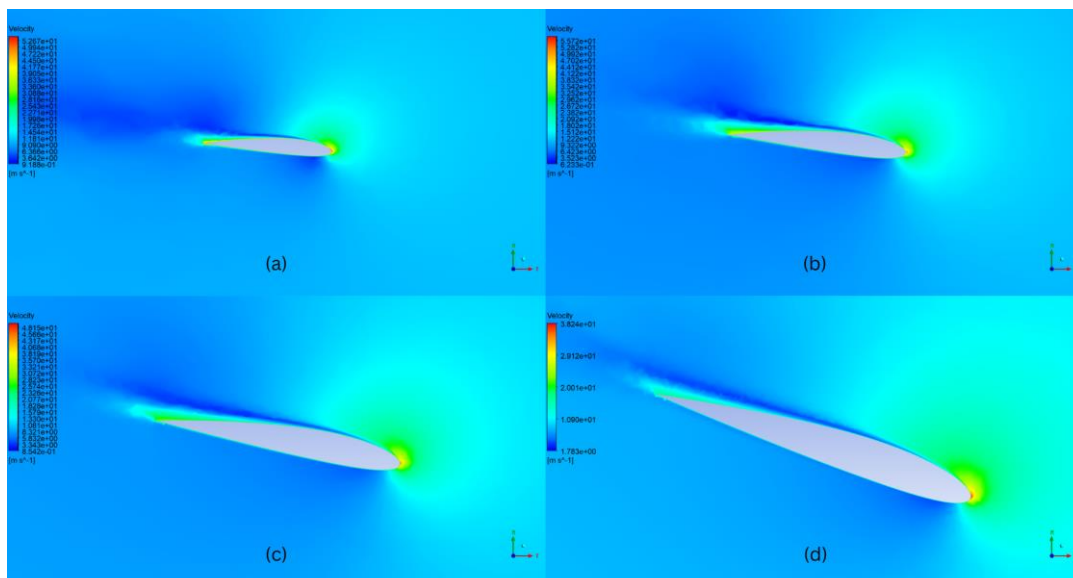


Fig. 7. Velocity contours on 3 blades a. R/r 1m b. R/r 0.75 m c. R/r 0.5 m d. R/r 0.25 m

3.3.2. Effect of Number of Blades on Vortex Formation

The vortex visualization (Figure 8-9) reveals significant differences between 3- and 4-blade turbines. The 4-blade turbine produces denser vortices in the tip region, especially at $R/r > 0.75$ m, which increases tip losses by up to 12% [13]. These vortices cause kinetic energy

dissipation and decrease the adequate pressure in the blade tail region, thus reducing the power coefficient (C_P) at $TSR > 6$. In contrast, the 3-blade turbine exhibits a more controlled vortex pattern, supporting higher efficiency.

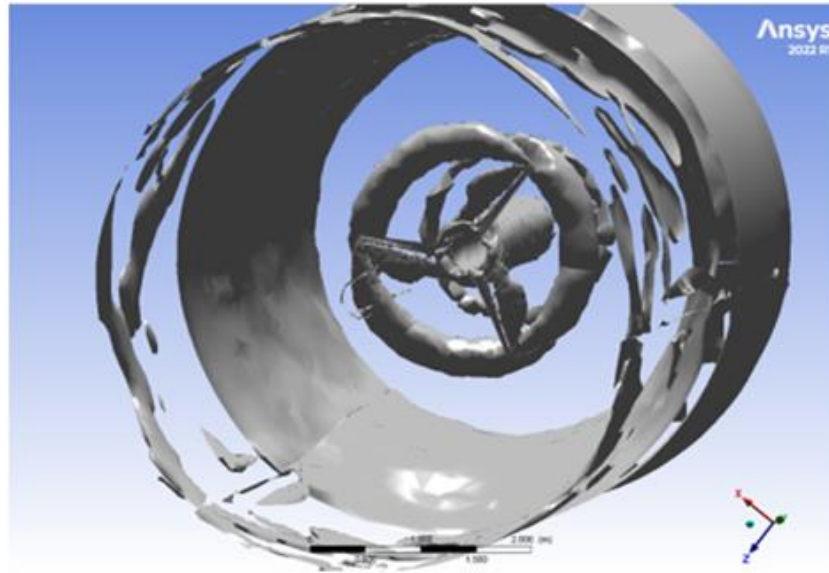


Fig. 8. Visualization of the vortex on NACA 0012 3-blade turbine

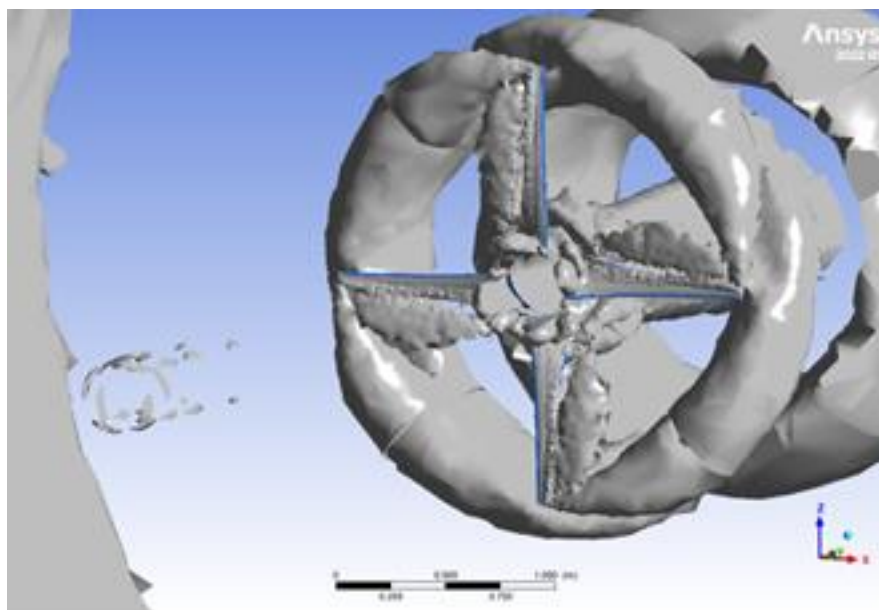


Fig. 9. Visualization of the vortex on NACA 0012 4-blade turbine

3.3.3. Number of Blades and Design Optimization

The 3-blade configuration has proven more efficient on the TSR 7 due to its even aerodynamic load distribution, avoiding the inter-blade flow interference often occurring in 4-blade turbines. Progressive twist angle optimization on three blades also reduces stall risk by maintaining the ideal angle of attack (α) along the blade, pushing C_P to 0.54 (close to the

theoretical Betz limit). On the other hand, the vortex density on 4 blades increases tip losses and widens the turbulence zone in the wake region, directly reducing the output power. These findings reinforce the importance of balancing the number of blades with local flow characteristics to minimize losses and maximize energy conversion.

4. CONCLUSION

This study successfully analyzed the effect of the number of blades on the performance of a low-scale NACA 0012 horizontal axis wind turbine (HAWT) using the Computational Fluid Dynamics (CFD) method. The simulation results showed that the 3-blade configuration produced the highest efficiency with a power coefficient (C_P) of 0.54 at a Tip-Speed Ratio (TSR) of 7, outperforming the 4-blade turbine which achieved a C_P of 0.48 at a TSR of 6. The mechanical power of the 3-blade turbine (1,040.81 W) was also 28% higher than that of the 4-blade turbine (927.28 W), confirming that fewer blades reduce inter-blade flow interference and tip losses due to vortex. The progressive distribution of twist angles on the 3 blades proved optimal in maintaining the ideal angle of attack ($\alpha=7.5^\circ$) along the blade, thereby minimizing the risk of stall and flow separation. CFD visualizations support these findings by showing a stable pressure gradient at the leading edge and a controlled vortex pattern, in contrast to a 4-blade turbine that produces dense vortices at the tip (Figures 8-9), increasing energy dissipation by up to 12% [13]. These findings are relevant to Indonesia's wind energy potential (speed 3-10 m/s), where a low-scale 3-blade turbine could be an efficient solution for remote island-based areas. Although the efficiency is still below the theoretical Betz limit (59.3%), the C_P result of 54% at 3 blades is close to the maximum optimization for practical scale. Further research can test variations in materials, blade geometry, and realistic wind conditions to expand the applicability of the design. Thus, this study provides a scientific basis for developing adaptive community wind turbines, supporting Indonesia's energy transition towards renewables.

ACKNOWLEDGEMENT

Thanks to Mr. Ahmad Alfarizi Barzah, S.T., who is the curator of this research.

REFERENCES

- [1] adi Ahdiat, "Konsumsi Listrik Penduduk Indonesia Naik pada 2022, Capai Rekor Baru," Databoks. Accessed: Apr. 23, 2024. [Online]. Available: <https://databoks.katadata.co.id/datapublish/2023/02/23/konsumsi-listrik-penduduk-indonesia-naik-pada-2022-capai-rekor-baru>
- [2] D. Kusdiana, "Laporan Kinerja Ditjen EBTKE 2022.," 2022. Accessed: Nov. 12, 2023. [Online]. Available: <https://www.esdm.go.id/assets/media/content/content-laporan-kinerja-direktorat-jenderal-energi-baru-terbarukan-dan-konservasi-energi-tahun-2022.pdf>
- [3] A. Praditya et al., "Indonesia Clean Energy Outlook Tracking Progress and Review of Clean Energy Development in Indonesia," Dec. 2019. [Online]. Available: www.iesr.or.id
- [4] P. Jamieson and Garrad. Hassan, *Innovation in Wind Turbine Design*, 1st ed. Chicaster, UK: A John Wiley & Sons, 2011. doi: 10.1002/9781119975441.
- [5] M. K. Johari, M. A. A. Jalil, and M. F. M. Shariff, "Comparison of horizontal axis wind turbine (HAWT) and vertical axis wind turbine (VAWT)," *International Journal of Engineering and Technology(UAE)*, vol. 7, no. 4, pp. 74–80, 2018, doi: 10.14419/ijet.v7i4.13.21333.
- [6] Kriswanto et al., "Rotor Power Optimization of Horizontal Axis Wind Turbine from Variations in Airfoil Shape, Angle of Attack, and Wind Speed," *Journal of Advanced Research in Fluid Mechanics and Thermal Sciences*, vol. 94, no. 1, pp. 138–151, 2022, doi: 10.37934/arfmts.94.1.138151.



- [7] H. Zhang, J. Wen, J. Zhan, and D. Xin, "Effects of blade number on the aerodynamic performance and wake characteristics of a small horizontal-axis wind turbine," *Energy Convers Manag*, vol. 273, p. 116410, 2022, doi: <https://doi.org/10.1016/j.enconman.2022.116410>.
- [8] A. Tummala, R. K. Velamati, D. K. Sinha, V. Indraja, and V. H. Krishna, "A review on small scale wind turbines," *Renewable and Sustainable Energy Reviews*, vol. 56, pp. 1351–1371, Apr. 2016, doi: [10.1016/j.rser.2015.12.027](https://doi.org/10.1016/j.rser.2015.12.027).
- [9] M. N. Kaya, F. Kose, D. Ingham, L. Ma, and M. Pourkashanian, "Aerodynamic Performance of a Horizontal Axis Wind Turbine with Forward and Backward Swept Blades.," *Journal of Wind Engineering and Industrial Aerodynamics*, vol. 176, pp. 166–173, May 2018, doi: [10.1016/j.jweia.2018.03.023](https://doi.org/10.1016/j.jweia.2018.03.023).
- [10] K. Deghoum *et al.*, "Optimization of Small Horizontal Axis Wind Turbines Based on Aerodynamic, Steady-State, and Dynamic Analyses," *Applied System Innovation*, vol. 6, no. 2, Apr. 2023, doi: [10.3390/asi6020033](https://doi.org/10.3390/asi6020033).
- [11] T. Burton, N. Jenkins, D. Sharpe, and E. Bossanyi, *Wind energy handbook*. John Wiley & Sons, 2011.
- [12] K. Oukassou, S. El Mouhsine, A. El Hajjaji, and B. Kharbouch, "Comparison of The Power, Lift and Drag Coefficients of Wind Turbine Blade from Aerodynamics Characteristics Of NACA 0012 and NACA 2412.," in *Procedia Manufacturing*, Tetouan, Moroco: Elsevier B.V., 2019, pp. 983–990. doi: [10.1016/j.promfg.2019.02.312](https://doi.org/10.1016/j.promfg.2019.02.312).
- [13] L. Qunfeng, C. Jin, and C. Jiangtao, "Study of CFD Simulation of a 3-D Wind Turbine," *China National Nature Science Fund*, vol. 5, no. 5, May 2011, doi: [10.1109/ICMREE.2011.5930883](https://doi.org/10.1109/ICMREE.2011.5930883).
- [14] A. Sayma, *Computational Fluid Dynamics*, 1st ed. London: Abdulnaser Sayma & Bookboon.com, 2009. Accessed: Apr. 24, 2024. [Online]. Available: <https://bookboon.com/en/computational-fluid-dynamics-ebook?mediaType=ebook>